Advanced Nano Research
Volume 8, Issue 1, pp. 1-17, 2025
DOI: https://doi.org/10.21467/anr.8.1.1-17
ISSN: 2581-5164
RESEARCH ARTICLE

Exploring Extracellular Vesicles Nanocapsules in Hydrogel Delivery for Canine Atopic Dermatitis: An Anti-Inflammatory Approach

Dutra, JMF[1*§], Dantas FML[2*§] Winck CP[1], Alberto AVP[2], Way DV[2], Motta AC[2], Oliveira ES[2], Nápole ML[1,3], Silveira JC[4], Lo Turco EG[1,5]

[1]Medmep
[2]Division of Materials / Instituto Nacional de Tecnologia - INT
[3]Chemsource
[4]Universidade de São Paulo
[5]Universidade Federal de São Paulo- Departamento de Cirurgia - Disciplina de Urologia

§ Both authors contribute equally

[*]Corresponding author's email: juliana.dutra@medmep.com / fabio.dantas@int.gov.br

Received: 17 May 2024 / Revised: 31 October 2024 / Accepted: 07 November 2024 / Published: 05 December 2024

ABSTRACT

This study aims to evaluate the anti-inflammatory potential of nanoencapsulated extracellular vesicles (EV) derived from canine mesenchymal stem cells (MSCs) in treating atopic dermatitis. It seeks to determine the efficacy of these EV in modulating cytokine responses, specifically targeting IL-2, IL-4, IL-5, IL-6, IL-10, IL13, and IL-31, which are crucial in the pathophysiology of cutaneous inflammatory disorders. Materials and Methods: MSCs were cultured from adipose tissue and induced to produce EVs. They were then isolated through ultracentrifugation, characterized for particle size and morphology, and encapsulated within calcium alginate nanogels. The anti-inflammatory activity was assessed in vitro using human keratinocyte cultures primed with IFN-gamma and treated with both free and nanoencapsulated EV. The expression of inflammatory cytokines was analyzed through RTq-PCR and protein ELISA Multiplex (Luminex®). Results: The study found that both free and nanoencapsulated EV significantly reduced the expression of IL-2, IL-4, IL-5, IL6, IL-10, IL-13, and IL-31 in IFN-gamma primed keratinocytes. Nanoencapsulation with alginate notably enhanced the delivery efficiency, targeted release, and stability of the EV, leading to a more pronounced reduction in cytokine expression compared to free EV. Conclusion: Nanoencapsulated EV derived from canine MSCs demonstrate significant anti-inflammatory potential, offering a promising therapeutic strategy for atopic dermatitis and other inflammatory conditions. This approach not only preserves the bioactivity of EV but also improves their therapeutic applicability through enhanced delivery and stability. The findings underscore the potential of nanoencapsulation technology in advancing novel therapeutic strategies across human and veterinary medicine, highlighting the importance of cross-disciplinary research in developing effective healthcare solutions.

Keywords: mesenchymal stem cells, extracellular vesicles, canine atopic dermatitis.

1 Introduction

Canine atopic dermatitis, a prevalent genetic and chronic condition, poses a significant concern for the well-being of pups, afflicting approximately 15% of the global canine population and dramatically compromising their quality of life due to relentless pruritus [1]. This multifaceted disorder instigates alterations in the epidermal layers, leading to persistent inflammation and skin lesions, often predisposing affected dogs to recurrent infections. The International Committee on Allergic Diseases of Animals (ICADA) suggests a new definition to canine atopic dermatitis in 2023 as "*Canine atopic dermatitis is a hereditary, typically pruritic and predominantly T- cell driven inflammatory skin disease involving interplay between skin barrier abnormalities, allergen sensitization and microbial dysbiosis*" [2]. What exacerbates the gravity of atopic dermatitis is its continual expansion, attributed to the ongoing exposure of cubs to environmental allergens that serve as potent

triggers for protracted inflammatory responses [3]. The treatment of atopic dermatitis in dogs typically involves a multifaceted approach, incorporating the use of shampoos, as well as steroidal and non-steroidal anti-inflammatory drugs (NSAIDs). Among the NSAIDs used in the systemic treatment of atopic dermatitis, meloxicam, and piroxicam are well-tolerated by pups, as demonstrated in a study by Niza et al. [4]. However, a challenge in their long-term use is the diminishing efficacy over time. The use of corticosteroids, while effective in alleviating symptoms, presents a significant drawback due to the potential for a range of adverse side effects, some of which can be life-threatening, as noted by Zanon et al. [5], making prolonged corticosteroid treatment impractical and risky. In response to these limitations, alternative therapies have emerged. Recent research, such as the study conducted by Kim et al. [6], has explored the potential of mesenchymal stem cells derived from various sources, including the umbilical cord, bone marrow, or adipose tissue, to suppress the allergic processes underlying atopic dermatitis, offering promising avenues for more effective and safer long-term treatment strategies. In pups, horses, cats, and most domestic animals, mesenchymal stem cells can be isolated from the spine cord [7], adipose tissue, synovial fluid, or umbilical cord [8]. The most used lineage is derived from adipose tissue due to the facility of acquisition.

The secretory capacity of mesenchymal stem cells derived from adipose tissue is not limited to the release of soluble factors such as TGF-β, IDO, EPG2, IL-10, and TNF. These cells can transfer molecules through the secretion of extracellular vesicles, which derive from the plasma membrane by budding and carry miRNA, mRNA, and proteins, protected by a lipid envelope [9]. In this sense, EVs emerge as potential vehicles to promote anti-inflammatory activity instead of stem cell therapy. They consist of small vesicles that act as messengers and transfer biomolecules naturally encapsulated in them, such as proteins and RNA, to regulate the functions of neighboring cells [10]. Results show that EVs can improve wound healing and facilitating skin regeneration, as they transport miRNAs, mRNAs, and proteins that can regulate signaling pathways in target cells [10-11]. EV extracted from mesenchymal stem cells from bone marrow, adipose, and placental tissues have been extensively studied for the treatment of various diseases. However, maintaining the stability of these EVs after injection in vivo remains one of the biggest challenges of these new cell- free therapies [12]. When ministered via subcutaneous, intraperitoneal, or intravenous injection, EVs accumulate in the liver, spleen, lung, or gastrointestinal tract and are destroyed in about 2 hours. In topical ministrations, sweat, tears, and exposure to external factors can hinder therapeutic action [13]. In the case of veterinary application, the physical removal itself through licking can hinder the treatment. In this sense, the association of EVs with hydrogels appears as an alternative to overcome these obstacles [11]. The use of hydrogels can also bring benefits in terms of protection and stability of the vesicles, increasing the product's lifetime and allowing the use of milder storage. Thus, encapsulating EVs in calcium alginate nanoparticles seems to be in every sense an intelligent route for applying these products to animals.

Calcium alginate is a biopolymer from genera *Laminaria*, *Macrocystis*, and *Ascophyllum nodosum* that consists of a linear chain of β-D-mannuronic acid and α-L-guluronic acid copolymers. Calcium alginate is generally biocompatible, meaning it can be safely used in contact with biological tissues. It is biodegradable, eventually breaking down into natural components. The strength of the alginate gel can be controlled by adjusting the concentration of alginate and calcium ions. The reaction between alginate and calcium ions is very quick. When calcium ions are added to a solution of sodium alginate, a cross-linking reaction occurs, resulting in a three-dimensional gel structure called egg-boxes that involve and protect the involucre [13,14]. Moreover, Sodium alginate is also approved for human use by the FDA (Food and Drug Administration) and is listed as a generally recognized as safe (GRAS) food additive, just like calcium alginate. This means it can be used in various food and cosmetic products without the need for prior approval. (eCFR :: 21 CFR 184.1724 Sodium alginate).

This research investigates the anti-inflammatory potential of EVs extracted from canine mesenchymal stem cells, encapsulated within calcium alginate nanogels. Despite the numerous benefits offered by nanogel encapsulation, a significant challenge remains in preserving the bioactivity of EVs postencapsulation. Our

methodology evaluates this by quantifying the reduction in inflammatory interleukins in human keratinocytes stressed with gamma interferon and pre-treated with these nanoencapsulated EVs. This approach not only tests the viability of using nanogel technology for EVs delivery but also explores the therapeutic efficacy of these vesicles in modulating inflammatory responses at a cellular level.

2 Materials and Methods

2.1 Mesenchymal stem cell culture (MSC)

MSC cryovial from adipose tissue was removed from the cell bank and immediately placed in the water bath, making circular movements, until the total thawing of the volume contained in the cryotube. In unidirectional flow, add FBS and culture medium to the cryovial and mix slowly. Gently transfer the entire contents of the cryotube to the 15 mL tube and centrifuge for 5 minutes. Discard all supernatant and dilute the cell pellet in 1 mL of IMDM culture medium (GIBCO) supplemented with 20% FBS. Keep the culture flasks at 37ºC and 5% CO_2 for 48 hours, at which time the first culture medium change is performed. The cells must remain in culture until they reach about 80 to 85% of confluence in the flasks, to start conditioned medium production.

2.2 Extracellular vesicle isolation

EVs were obtained from the conditioned MSC culture medium through ultracentrifugation. To this end, the MSC conditioned medium was centrifuged at 300xg for 10 minutes to remove cells, 2,000xg for 10 minutes to remove cell debris, and 16,500xg for 30 minutes to remove larger extracellular vesicles. Centrifuges were carried out at a temperature of 4°C. To obtain content enriched in EVs smaller than 200 nm, the fluid was filtered through a filter with a 0.22μm pore size (Kasvi- Brazil) and ultracentrifuged at 119,700 xg for 70 minutes at 4°C (Optima XE-90 Ultracentrifuge; rotor 70 Ti; Beckman Coulter). After the first ultracentrifugation, the pellet was diluted in phosphate- buffered saline (PBS) and ultracentrifuged again at 119,700 xg for 70 minutes at 4°C. The pellet obtained was diluted in 50 μL of calcium and magnesium-free PBS. Particle size analysis and concentration were done with EVs isolated from MSC culture medium and diluted in 50 μL of magnesium-calcium-free PBS using the Nanosight device (NS300; NTA 3.1 Build 3.1.45; Malvern). The dilution factor used for reading was 1:500 in PBS. Five 30- second videos were taken, captured by the sCMOS camera on Level 15 Camera and temperature controlled at 37 °C.

The morphology of EVs was done using SEM (Scanning Electronic Microscopy) and TEM (Transmission Electronic Microscopy). For SEM, the methodology used was described by Faruqu [13] A sample of EVs was fixed in 5% glutaraldehyde for 2 h, which was then added on the surface of aminopropyltrimethoxysilane (APTES, 1% w/v ethanol/water 19:1) pre-treated silicon wafer and left for 1 h. This was followed by washing with PBS three times and dehydrating in a series of increasing ethanol concentrations (20, 50, 70, 90, 95, 100%). The samples were transferred for critical drying (EM CPD030 Leica), and sputter coated with gold before scanning. SEM was performed on QUANTA FEG 450 (FEI) operated at 20 kV. For TEM, was used an FEI Tecnai T20 and the sample of exosomes was fixed firstly in paraformaldehyde (2% w/v) and applied over 200 mesh copper grids Formar carbon coated. Using the dropover Parafilm methodology, the cooper grid was washed in the sequence PBS buffer, glutaraldehyde (1%. v/v), and deionized water. After that, negative staining was achieved the grid was embedded using uranyl acetate (4%) in methylcellulose solution (2%) 1:9 for 10 min and left to air-dry.

For EVs inside nanoparticles, it was used immunocytochemistry to observe the completeness of the phospholipid layer. Nanocapsules loaded with EVs were fixed with paraformaldehyde 2% diluted in phosphate saline buffer for 5 minutes. They were allowed to adhere in 200 mesh copper grids covered in FORMVAR ® for 5 minutes at 4°C. For blocking free aldehyde groups, grids were treated with 0.05M of glycine for 10 minutes and transferred to 1%BSA PBS solution for 30 minutes. Antibody anti-CD41A (1:1000 in PBS 0.1% BSA) was incubated for 1 hour at 4°C in. The grids were washed and posterior

incubated with anti-mouse IgG 10 nm colloidal gold 1:500 in PBS/BSA solution. Wash the grids in separate drops of (50 µL) PBS 0.1% BSA for 10 min each. Wash the grids in 2 drops of distilled water before proceeding to negative counterstaining with 2% uranyl acetate proceed to 80Kv TEM.

2.3 Extracellular vesicles nanoencapsulation

The entire process was carried out with sterilized materials and reagents, as described. At first, it was prepared 10 mL of 0.225 mol/L $CaCl_2.2H_2O$ (Chemicals) solution. Also, it was prepared 10 mL 5% (w/V) solution of polyvinylpyrrolidone (Aldrich) with Mw=10,000 (PVP-10). After that, it was prepared 10 mL of 1% sodium alginate (FMC) solution. All solution was filtered through a 0.45 µm syringe filter and stored in an autoclaved bottle with a lid. For phase A preparation, at last, 0.16 g of Tween 80 (Sigma-Aldrich) was mixed with 64 ml of isopropanol in an autoclaved glass beaker with a capacity of 250 mL. Then, it was put in 8ml PVP-10/$CaCl_2$ solution and was blended for 30 sec under a water bath at 20ºC. In phase B preparation, around 400 µL of extracted EVs was separated and then added to 10 mL of sodium alginate solution and stirred to homogenize the mixture well. During the final mixing, phase B was dripped slowly into phase A under ultra-disperser at 15,000 rpm. Throughout the process, control the temperature inside the beaker so that it has remained within the range of 20-25°C. The nanoparticle was recovered using a centrifuge at 4500 rpm at 4°C for 10 min. The settle was washed with isopropanol to remove all remaining supernatant from the mixture batch. The procedure was repeated two more times. The isopropanol-embedded nanoparticles had their morphology analyzed by MET, MEV, and Multiplexing assay.

2.4 Extracellular vesicles content analysis

For the evaluation of the anti-inflammatory citokines in the EVs a multiplex assay was performed by Bio-Plex 200 Systems (Bio-Rad). It was used the ProcartaPlex™ Canine Cytokine/Chemokine/Growth Factor Panel 1, 11plex from ThermoFisher (catalog: EPX11A-50511- 901). Briefly, the isolated EVs and encapsulated EVs were lysed by adding 100 µL of protein lysis buffer (RIPA, Sigma-Aldrich) for 20 minutes on ice, followed by 10 minutes of sonication. The extracts were removed from the microtube, passed through an insulin syringe five times, and centrifuged at 14,000 x g for 15 minutes at 4 °C. A protease inhibitor cocktail (Sigma-Aldrich) was added to the proteins collected and stored at -70°C. The multiplex assay was done according to the manufacturer's instructions.

2.5 Anti-inflammatory activity in stimulated keratinocyte culture

Keratinocyte cell cultures were maintained with DMEM (Dulbecco's Modified Eagle's Medium - Gibco) with the addition of 10% fetal bovine serum at 37°C and 5% CO_2. For each condition tested, cells were allowed to grow in a 24-well plate 24 hours before stress conditions. The next day, interferon 10ng/mL was added to simulate the condition of cellular stress for 24 hours (Ha et al,. 2020). The cells were divided in groups according to the table 1 below:

Table 1: *Samples groups for each condition tested during anti-inflammatory activity in stimulated keratinocyte culture*

Positive control	IFN-g 24h + dexametasone
Negative control	IFN-g 24h + sodium lauryl sulfate
Interferon Control	IFN-g 24h
Control	Culture medium
Sample NV.1305.02	Nanoencapsulation EVs
Sample NV.1436.02	Nanoencapsulation EVs
Sample NV.1437.02	Nanoencapsulation EVs
Sample NV.1304.02	EVs
Sample NV.1303.02	EVs

The solutions containing the control and sample groups were applied to the keratinocyte cell culture followed by incubation at 37°C and 5% CO_2 for 48 hours. Afterwards, messenger RNA was extracted with Trizol, evaluated its quantity and purity. From the messenger RNA, the reverse transcriptase reaction was used to obtain the complementary DNA strand. Next, analysis of the expression of genes related to inflammation (IL-2, IL-4, IL-5, IL-6, IL-10, IL-13 and IL-31) was performed. The GAPDH marker was used as endogenous control. Assessment of markers by reverse transcriptase reaction followed by real-time polymerase chain reaction (RTq-PCR) performed by Quant3. The results were evaluated using Microsoft Excel software and GraphPad Prism. For the analysis of data obtained by RTq-PCR, we used analysis from 2-ΔΔCt for a graphical representation of the relative expression by fold-change and statistical analysis based on Δ Ct data. Analysis statistics for comparison between groups was performed using a One-way test Anova with Bonferroni post-test and the level of statistical significance was considered less than 0.05.

3 Results and Discussion

3.1 Extracellular vesicles and nanoencapsulated physical analysis

The results from 3 different batches (AM4, AM5, and AM6) are shown in Fig. 1. The results indicate that all materials are mostly in the size range of 100 to 200 nm. Generally, EVs have size ranges 50- 150 nm [14-16]. Also, the NTA analyses carried out indicate, at least, 10^8 particles/mL.

(a)

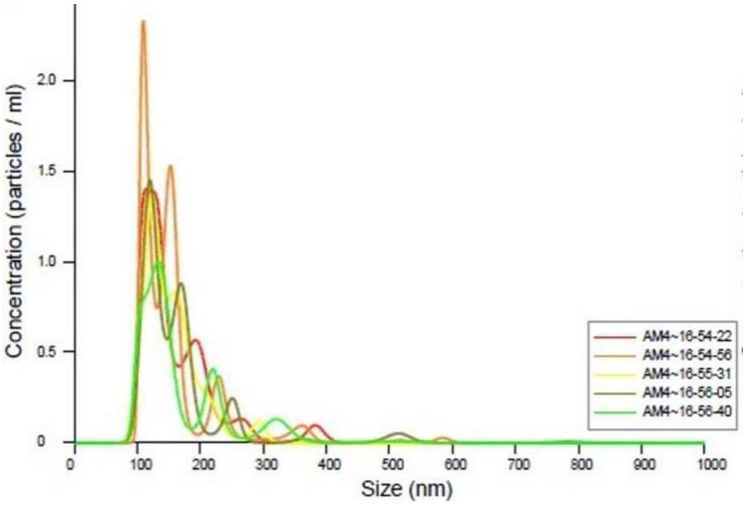

Concentration:
9.68e+08 +/- 5.59e+07 particles/ml
52.9 +/- 3.1 particles/frame
54.1 +/- 3.0 centres/frame

(b)

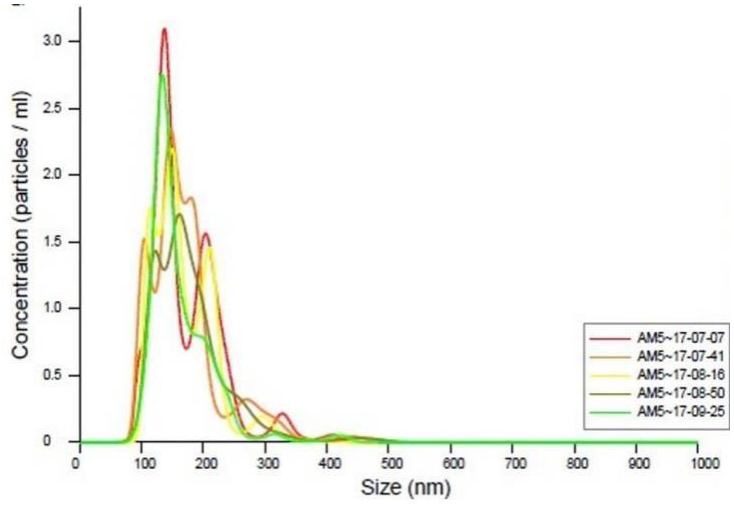

Concentration:
2.01e+09 +/- 9.67e+07 particles/ml
109.8 +/- 5.3 particles/frame
113.9 +/- 5.9 centres/frame

(c)

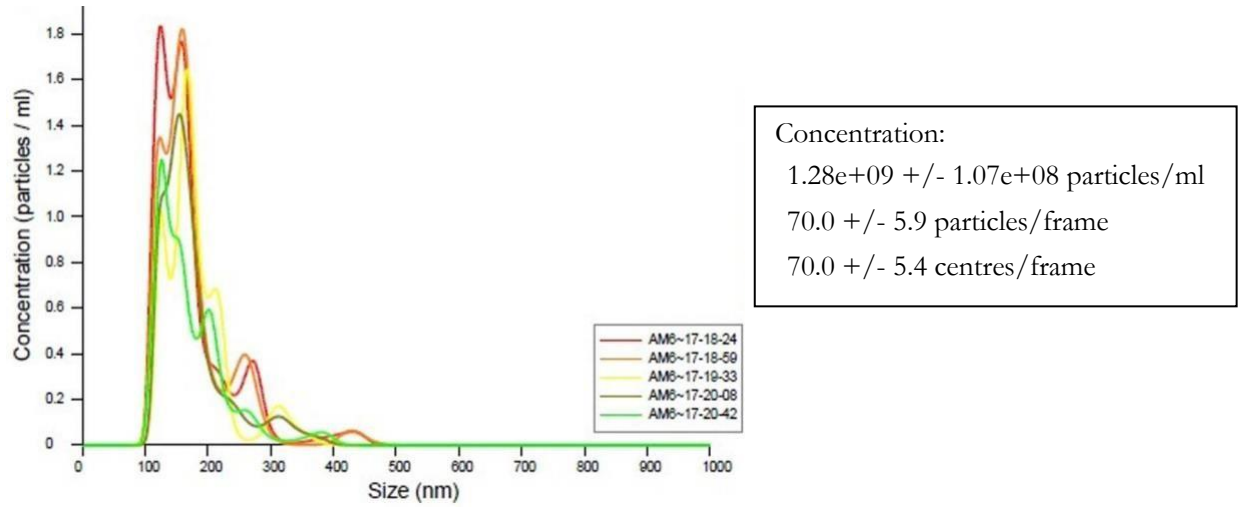

Figure 1: ***(a)*** *EV sample AM4;* ***(b)*** *EV sample AM5;* ***(c)*** *EV sample AM6*

In Fig. 2(a1), it is possible to view an SEM image of the EV that shows the presence of multiple vesicles ranging in size from 49 to 120nm (Fig. (a2)) and morphology semi-spherical. When comparing the NTA data, it is evident that in microscopy analyses the average sizes are smaller. However, the sample preparation process for SEM involves prior fixation of EV with a glutaraldehyde solution, which causes the vesicles to shrink. It is not observed any disrupted structure of EV.

In Fig.2 (b1), we can see the nanoencapsulated material having very spherical morphology and no agglutination. The size distribution range between 150 to 350nm.

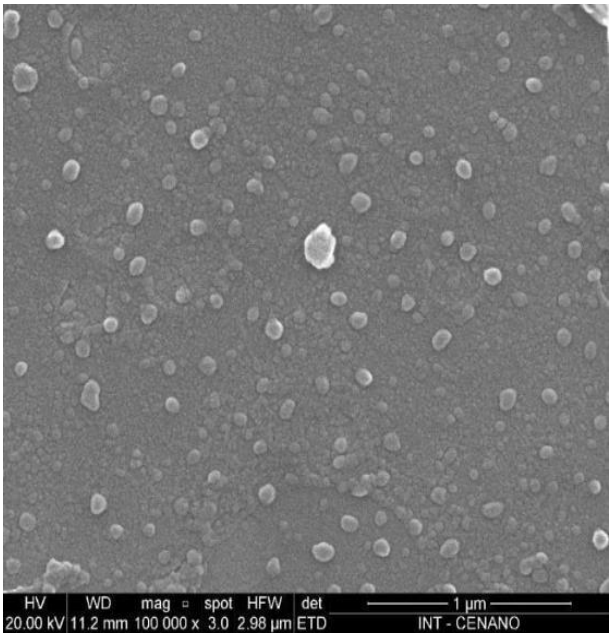

(a1)

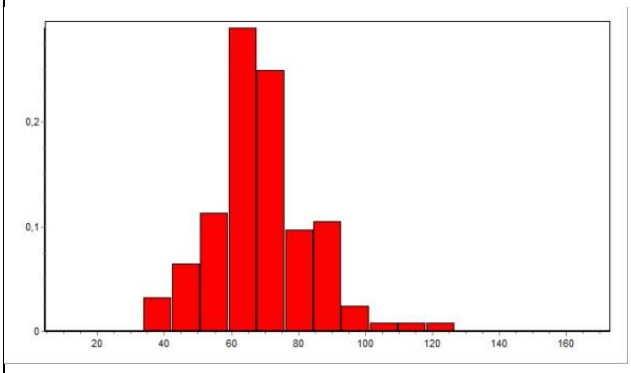

(a2)

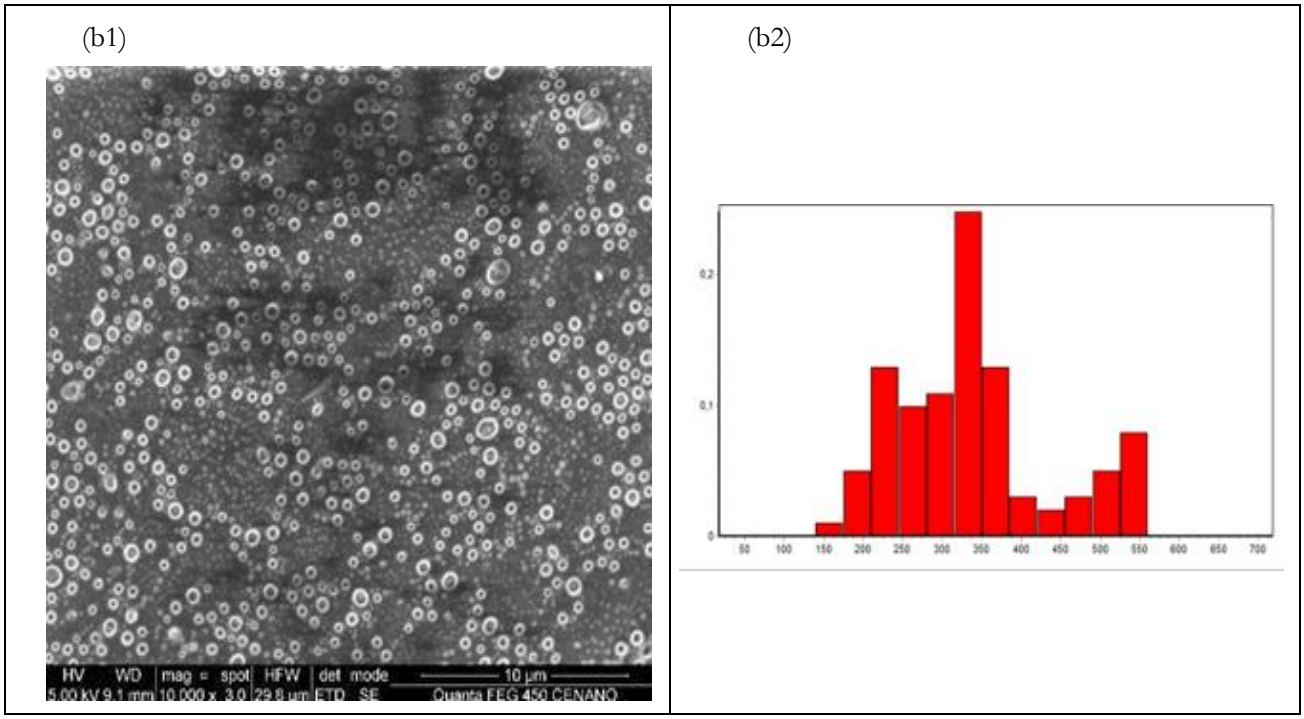

Figure 2: *SEM images for* ***(a)*** *EV, 20kV, 100,000x*
(b) *Nanoencapsulated EV, 3 kV, 10,000x, and size particle analysis distribution respectively*

Fig. 3(a) shows the vesicles stained with uranyl acetate. As in the case of SEM analyses, the shrinkage of the particles caused by the glutaraldehyde fixation process, necessary to provide greater rigidity to the EVs, as already mentioned, was noted. It is not possible to identify degraded vesicles or structure disruption.

Fig. 3(b) shows clearly the encapsulation of EV by calcium alginate, but few particles are empty. In Fig. 3(c), we can see amplified microscopy of nanoencapsulated EVs. In this case, nanocapsules have a size naturally bigger for EV entrapment, and the same aspect was found in the SEM analysis, Fig 2b.

(a)

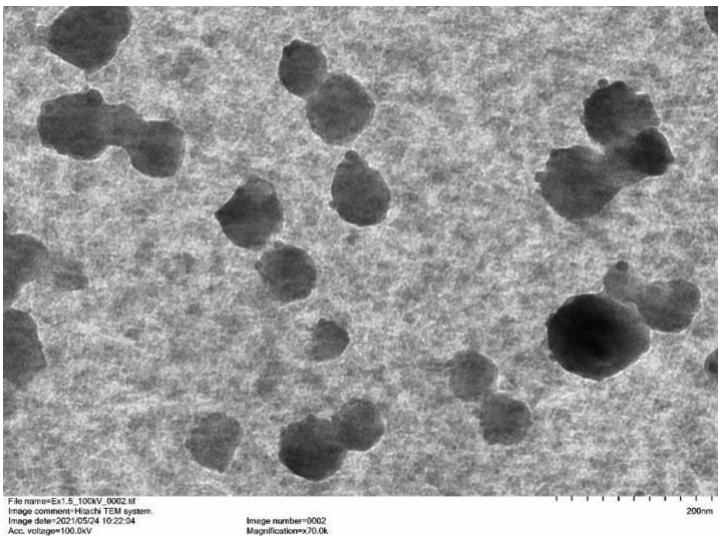

(b)

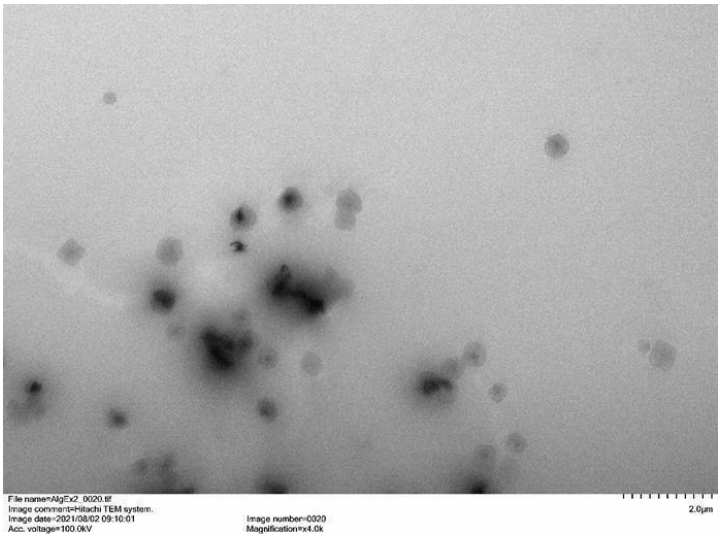

(c)

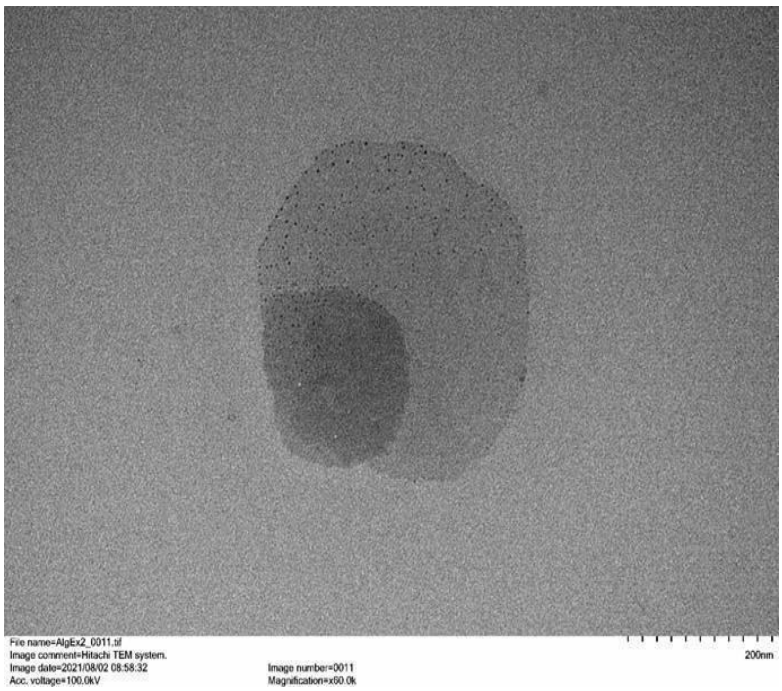

Figure 3: ***(a)*** *EV TEM;* ***(b)*** *Nanoencapsulated EV TEM and* ***(c)*** *Amplified size of nanoencapsulated EV TEM.*

From Figure 4, the samples observed under the transmission electron microscope showed positive staining for anti CD-41A, that is, the EVs have their membrane preserved even inside the alginate nanocapsule. Both the negative control and the secondary antibody control showed no labeling, which validates the labeling found in samples incubated with anti CD 41.

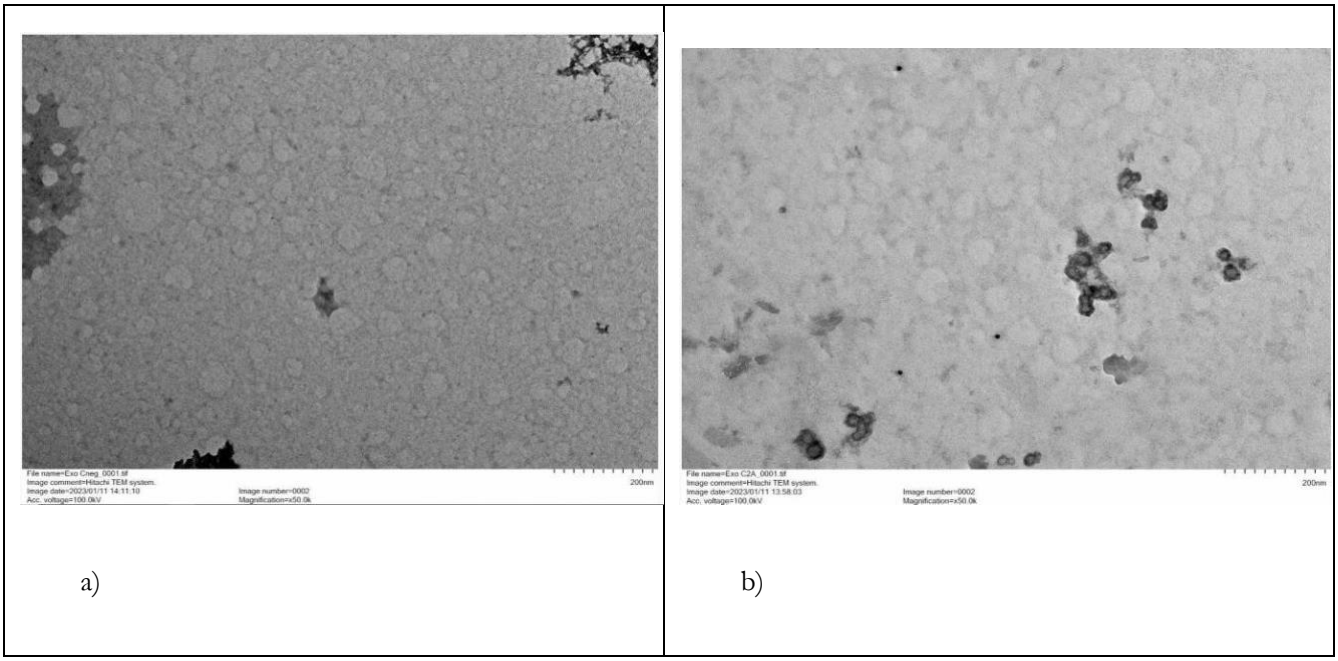

Figure 4: *Anti-CD 41 localization by TEM to study the phospholipid layer.* ***a)*** *TEM from extracted EVs – Negative control;* ***b)*** *TEM from extracted EVs – Positive control*

3.2 Nanoencapsulation of extracellular vesicles and cytokines analysis

Figure 5 shows results from multiplex assay from EVs and nanoencapsulated one in two physical states, lyophilized and gelatinized. Eleven cytokines were evaluated IFN-ɣ, IL-10, IL-12, IL-23P40, IL- 6, IL-8, MCP-1, NGF-β, SCF, TNF-α, VEGF-A. All samples had the 11 searched cytokines but at different concentrations. However, the IFN-ɣ presented concentrations higher than the standard curve of the equipment and it was inviable to analyze it. Except for VEGF-A, no sensible difference is observed among the samples. The multiplex assay results show that the encapsulated EVs do not suffer degradation by the encapsulation process used since all determined cytokines are found in the products. Despite the large variation in measurements, the mean and standard deviation of the cytokine concentration indicate that the encapsulation efficiency can be considered 100% in the two analyzed systems overlaps, so we can consider that statistically 100%. Now, to validate, we need a higher and/or even more sensitive methodologies. These findings were corroborated by functional assays (quantitative PCR of keratinocytes exposed to encapsulated and non-encapsulated exosomes), demonstrating that the encapsulated contents are performing as expected.

The next step in the study will be to conduct stability analysis under various physiological conditions.

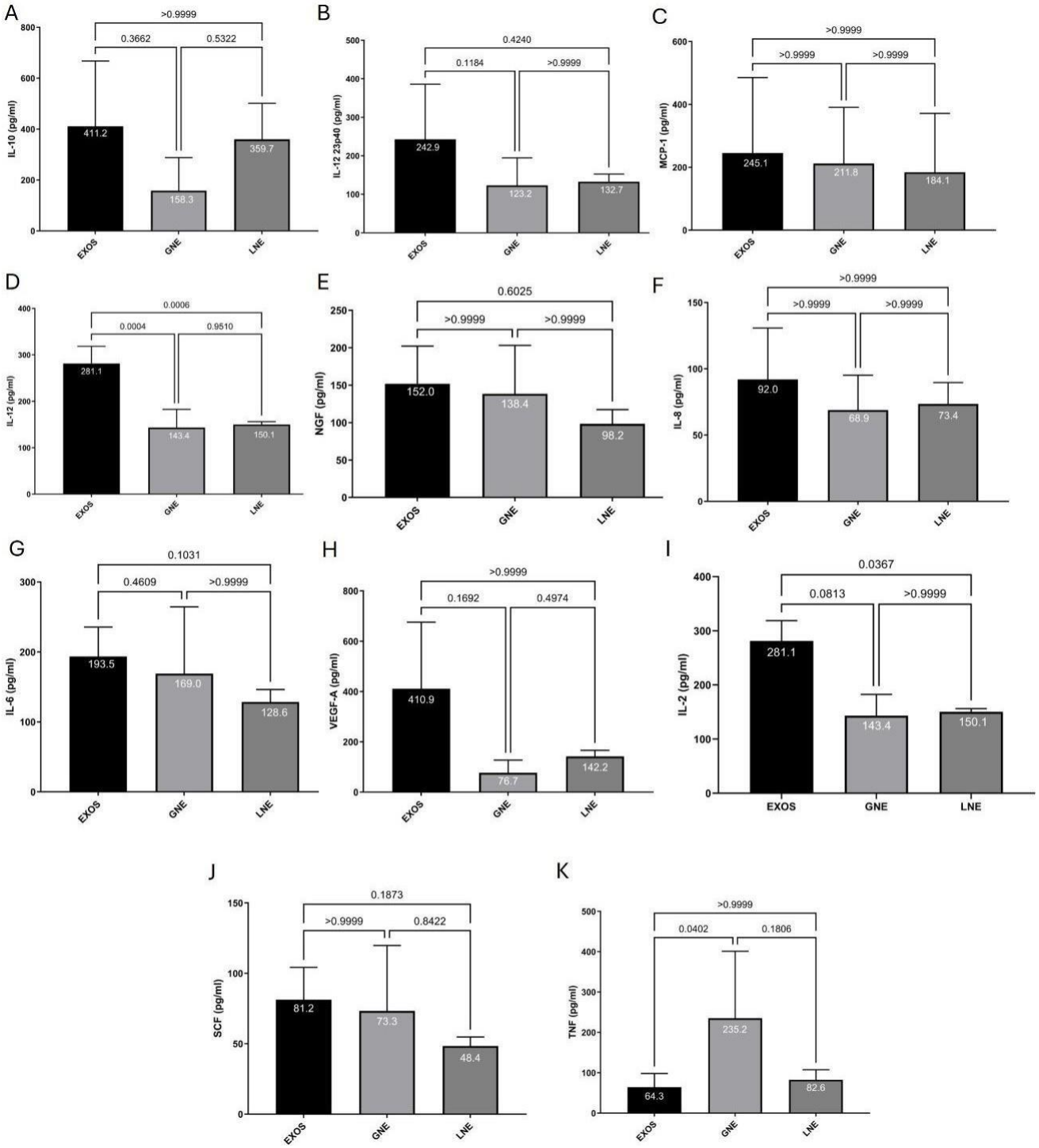

Figure 5: *EVs cytokine analysis performed by multiplex methodology for pure EV (EXOS), gelatinized nanoencapsulated EVs (GNE) and lyophilized nanoencapsulated EVs (LNE)*

3.3 Anti-inflammatory activity

To simulate inflammatory stress, keratinocyte cells were exposed to interferon for 24 hours. Then, the treatments with the negative control group (sodium lauryl sulfate), positive control (dexamethasone 20ug/mL), and with samples for nanoencapsulated EVs (NV.1305.02, NV 1436,02, NV 1437.02), and isolated EVs (NV.1303.02 and NV.1305.02) for 48 hours. In our study, we utilized two internal controls as negative controls: SLS (Sodium Lauryl Sulfate) and IFN (Interferon) to trigger a pro-inflammatory state. Consequently, all treatment graphs were compared with the IFN control; however, they could also generally be compared with the SLS control. In both cases, the majority of the treatments were effective in reducing

cytokines. In relation to anti- inflammatory cellular studies, is usual to use dexamethasone as a positive control. Dexamethasone reduces the expression of pro-inflammatory cytokines such as IL-1, IL-6, and TNF-α, which are crucial in inflammatory responses. [16,17].

On the other hand, interferon gamma (IFN-γ) can simulate an inflammatory state in cell cultures. It is known to be a pro-inflammatory cytokine that can induce the expression of various cytokines and molecule adhesion, promoting an inflammatory response. In cell cultures, IFN-γ is often used to study immune response and inflammation mechanisms. [18]. Meanwhile, sodium lauryl sulfate is widely recognized for its irritant properties, making it a valuable tool in patch testing to evaluate skin sensitivity and barrier dysfunction. Studies indicate that SLS can enhance the penetration of allergens, potentially increasing the sensitivity of patch tests for allergic contact dermatitis [19-21]. At the end of treatment, analysis was carried out using the RTq-PCR technique in which expression was compared relative number of markers related to the inflammatory process (IL-2, IL-4, IL-5, IL-6, IL-10, IL-13, and IL- 31). In this report, the analysis was carried out using the normalization of the control group without exposure to interferon at 1.0 and the other groups compared to it. For IL-2 analysis, the interferon group demonstrated an increase of 2.32 (±0.08) times when compared to the control group. The negative control group demonstrated a 2.29-fold increase (±0.18) in the expression of this cytokine. The positive control group demonstrated a level of 1.29 (±0.44) about the control. Exposure to sample NV.1303.02 demonstrated a level of 0.87 times (±0.07) in IL-2 expression compared to the control group. In the comparison of the sample with the interferon group, exposure to the sample NV.1303.02 demonstrated a 62.1% reduction in the expression of this marker. An exposure to sample NV.1304.02 demonstrated a level of 0.57(±0.16) in the expression of IL-2 compared to the control group. When comparing the sample with the interferon group, exposure to sample NV.1304.02 demonstrated a reduction of 75.1% of the expression of this marker. Exposure to sample NV.1305.02 demonstrated a level of 0.62 (±0.06) in IL-2 expression compared to group control. When comparing the sample with the interferon group, the exposure to sample NV.1305.02 demonstrated a 73.2% reduction in the expression of that marker.

In this study, our primary focus was on analyzing the impact of interferon within the context of a control group. Notably, we found statistically significant differences among the treated groups, ng the efficacy of various interventions. These results are illustrated in Figure 6.

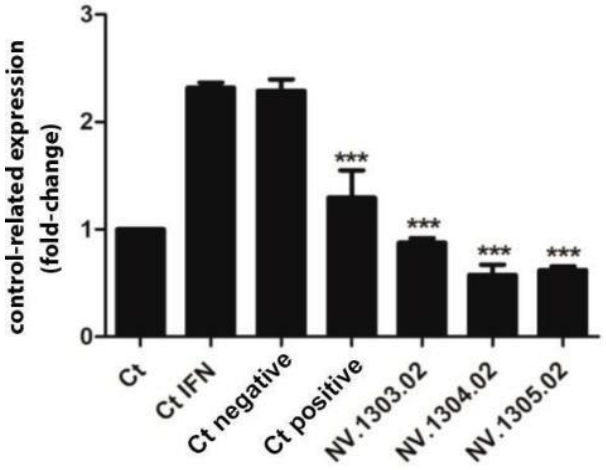

Figure 6: *Result of analysis of relative expression of IL-2 between groups. Horizontal bars connect the groups to demonstrate the level of statistical difference (***p<0.001).*

For IL-4 analysis, the interferon group demonstrated an increase of 2.12 (±0.26) times when compared to the control group. The negative control group demonstrated a 2.48-fold increase (±0.17) in the expression of this cytokine. The positive control group demonstrated a level of 1.5 (±0.17) concerning the control group. Exposure to sample NV.1303.02 demonstrated a 1.12-fold increase (±0.07) in IL-4 expression

compared to the control group. When comparing the sample with the interferon group, exposure to sample NV.1303.02 demonstrated a 46.7% reduction in the expression of this marker.

Exposure to sample NV.1304.02 demonstrated a 1.27-fold increase (±0.11) in IL-4 expression compared to the control group. When comparing the sample with the interferon group, exposure to sample NV.1304.02 demonstrated a 39.9% reduction in the expression of this marker. Exposure to sample NV.1305.02 demonstrated a 1.38-fold increase (±0.10) in IL-4 expression compared to the control group.

When comparing the sample with the interferon group, exposure to sample NV.1305.02 demonstrated a 34.6% reduction in the expression of this marker. The analysis presented is in relation to the control group with interferon. These results illustrated in Figure 7 showed that IL-4 expression was also reduced as IL-2 but at a lower rate.

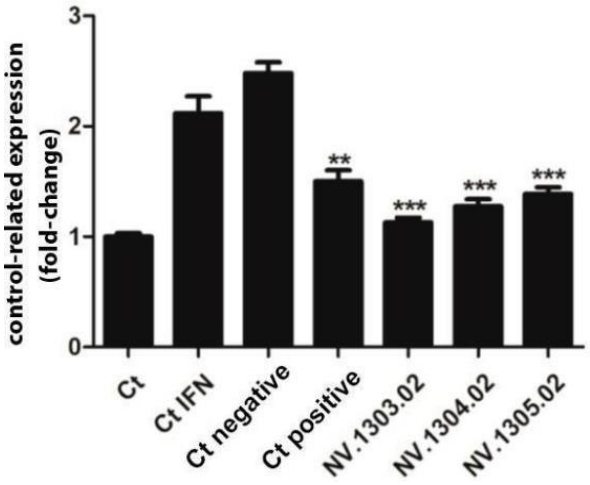

Figure 7: *Result of relative IL-4 expression analysis between groups. Horizontal bars connect the groups to demonstrate the level of statistical difference (***p<0.001).*

For IL-5 analysis, the interferon group demonstrated an increase of 1.78 (±0.32) times when compared to the control group. The negative control group demonstrated a 3.78-fold increase (±0.05) in the expression of this cytokine. The positive control group demonstrated a level of 1.33 (±0.05) in relation to the control group. Exposure to sample NV.1303.02 demonstrated a 1.47-fold increase (±0.001) in IL-5 expression compared to the control group. When comparing the sample with the interferon group, exposure to sample NV.1303.02 demonstrated a 17.1% reduction in the expression of this marker. Exposure to sample NV.1304.02 demonstrated a 1.74-fold increase (±0.10) in IL-5 expression compared to the control group. When comparing the sample with the interferon group, exposure to sample NV.1304.02 demonstrated a 2.22% reduction in the expression of this marker.

Exposure to the sample NV.1305.02 demonstrated a 1.66-fold increase (±0.17) in IL-5 expression compared to the control group. When comparing the sample with the interferon group, exposure to sample NV.1305.02 demonstrated a 6.3% reduction in the expression of this marker. When comparing the sample with the interferon group, exposure to sample NV.1303.02 demonstrated a 17.1% reduction in the expression of this marker. Exposure to sample NV.1304.02 demonstrated a 1.74-fold increase (±0.10) in IL-5 expression compared to the control group. When comparing the sample with the interferon group, exposure to sample NV.1304.02 demonstrated a 2.22% reduction in the expression of this marker. Exposure to the sample NV.1305.02 demonstrated a 1.66-fold increase (±0.17) in IL-5 expression compared to the control group. When comparing the sample with the interferon group, exposure to sample NV.1305.02 demonstrated a 6.3% reduction in the expression of this marker.

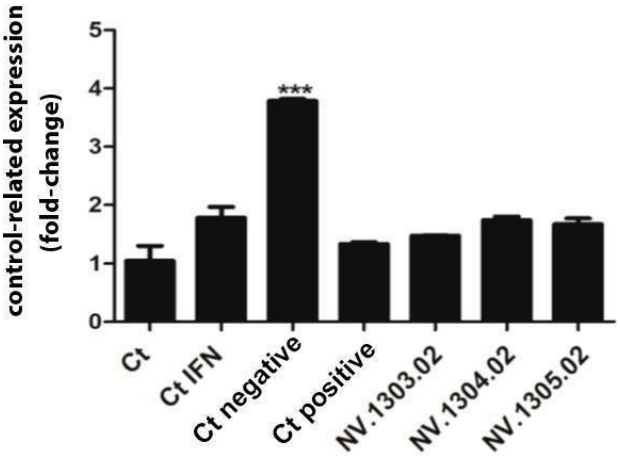

Figure 8: *Result of relative IL-5 expression analysis between groups. Horizontal bars connect the groups to demonstrate the level of statistical difference (***p<0.001).*

For IL-6 analysis, the interferon group demonstrated an increase of 1.5 (±0.18) times when compared to the control group. The negative control group demonstrated a 2.7-fold increase (±0.16) in the expression of this cytokine. The positive control group demonstrated a level of 1.29 (±0.08) in relation to the control group. Exposure to sample NV.1303.02 demonstrated a 1.2-fold increase (±0.007) in IL-6 expression compared to the control group. When comparing the sample with the interferon group, exposure to sample NV.1303.02 demonstrated a 19.5% reduction in the expression of this marker. Exposure to sample NV.1304.02 demonstrated a 2.13-fold increase (±0.02) in IL-6 expression compared to the control group.

When comparing the sample with the interferon group, exposure to sample NV.1304.02 demonstrated a 42.3% increase in the expression of this marker. Exposure to sample NV.1305.02 demonstrated a 1.36-fold increase (±0.13) in IL-6 expression compared to the control group. When comparing the sample with the interferon group, exposure to sample NV.1305.02 demonstrated a 9.22% reduction in the expression of this marker. See Figure 9

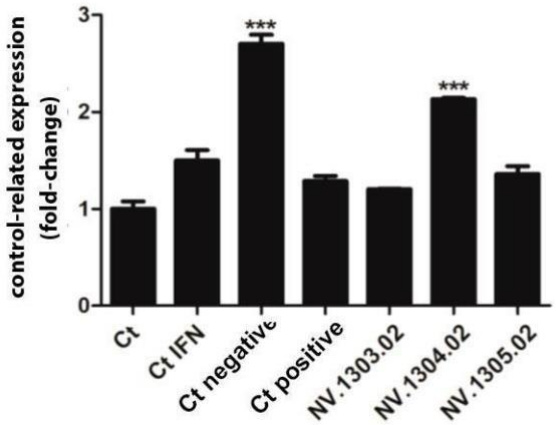

Figure 9: *Result of analysis of relative expression of IL-6 between groups. Horizontal bars connect the groups to demonstrate the level of statistical difference (***p<0.001).*

For IL-10 analysis, the interferon group demonstrated an increase of 2.98 (±0.12) times when compared to the control group. The negative control group demonstrated a 3.17-fold increase (±0.17) in the expression of this cytokine. The positive control group demonstrated a level of 0.94 (±0.36) in relation to the control group. Exposure to sample NV.1303.02 demonstrated a level of 0.84 (±0.05) in IL-10 expression compared to the control group. When comparing the sample with the interferon group, exposure to sample

NV.1303.02 demonstrated a 71.7% reduction in the expression of this marker. Exposure to sample NV.1304.02 demonstrated a level of 1.02 (±0.22) in IL-10 expression compared to the control group. When comparing the sample with the interferon group, exposure to sample NV.1304.02 demonstrated a 65.7% reduction in the expression of this marker. Exposure to sample NV.1305.02 demonstrated a level of 1.08 (±0.31) in IL-10 expression compared to the control group. When comparing the sample with the interferon group, exposure to sample NV.1305.02 demonstrated a 63.8% reduction in the expression of this marker. Figure 10.

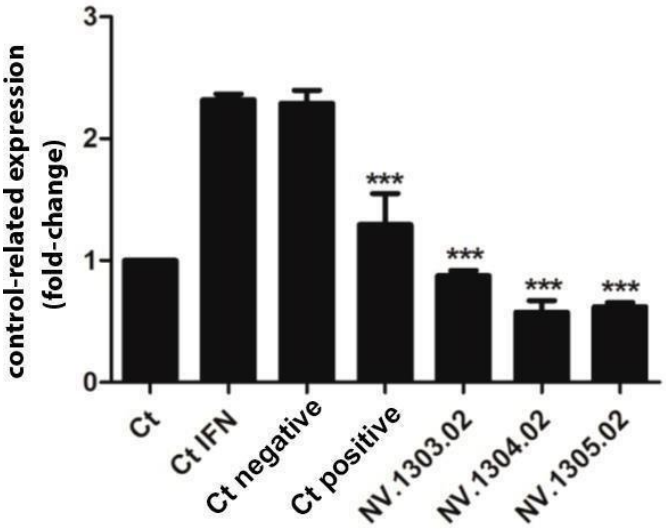

Figure 10: *Result of relative expression analysis of IL-10 between groups. Horizontal bars connect the groups to demonstrate the level of statistical difference (***p<0.001).*

For IL-13 analysis, the interferon group demonstrated an increase of 2.19 (±0.04) times when compared to the control group. The negative control group demonstrated a 3.04-fold increase (±0.21) in the expression of this cytokine. The positive control group demonstrated a level of 1.13 (±0.31) concerning the control group. Exposure to sample NV.1303.02 demonstrated a 1.14-fold increase (±0.18) in IL-13 expression compared to the control group. When comparing the sample with the interferon group, exposure to sample NV.1303.02 demonstrated a 47.6% reduction in the expression of this marker. Exposure to sample NV.1304.02 demonstrated a 1.15-fold increase (±0.05) in IL-13 expression compared to the control group. When comparing the sample with the interferon group, exposure to sample NV.1304.02 demonstrated a 47.1% reduction in the expression of this marker. Exposure to sample NV.1305.02 demonstrated a level of 1.1 (±0.6) in IL-13 expression compared to the control group. When comparing the sample with the interferon group, exposure to sample NV.1305.02 demonstrated a 49.6% reduction in the expression of this marker. See Figure 11.

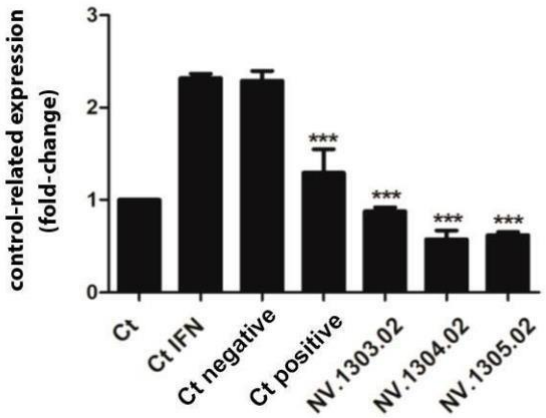

Figure 11: *Result of relative expression analysis of IL-13 between groups. Horizontal bars connect the groups to demonstrate the level of statistical difference (***p<0.001).*

For IL-31 analysis, the interferon group demonstrated an increase of 2.08 (±0.15) times when compared to the control group. The negative control group demonstrated a 2.58-fold increase (±0.38) in the expression of this cytokine. The positive control group demonstrated a level of 0.97 (±0.23) concerning the control group. Exposure to sample NV.1303.02 demonstrated a level of 0.49 (±0.008) in IL-31 expression compared to the control group. When comparing the sample with the interferon group, exposure to sample NV.1303.02 demonstrated a 76.3% reduction in the expression of this marker. Exposure to sample NV.1304.02 demonstrated a level of 0.32 (±0.03) in IL-31 expression compared to the control group. When comparing the sample with the interferon group, exposure to sample NV.1304.02 demonstrated an 84.5% reduction in the expression of this marker. Exposure to sample NV.1305.02 demonstrated a level of 0.6 (±0.07) in IL-31 expression compared to the control group. When comparing the sample with the interferon group, exposure to sample NV.1305.02 demonstrated a 70.7% reduction in the expression of this marker. See Figure 12.

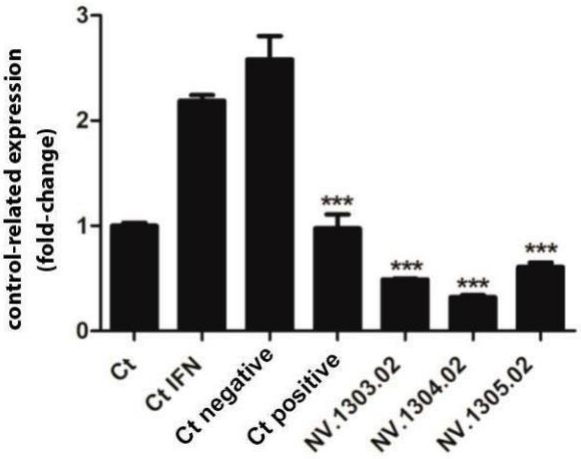

Figure 12: *Result of relative expression analysis of IL-31 between groups. Horizontal bars connect the groups to demonstrate the level of statistical difference (***p<0.001).*

4 Conclusion

Our investigation conclusively demonstrates the anti-inflammatory potential of nanoencapsulated EVs in modulating cytokine responses, specifically targeting IL-2, IL-4, IL-5, IL-6, IL-10, IL-13, and IL-31. These cytokines are notably implicated in the pathophysiology of cutaneous inflammatory disorders, such as atopic dermatitis. The study's in vitro analysis, involving human keratinocytes primed with IFN-gamma and treated with both isolated and nanoencapsulated EVs, revealed a significant reduction in the majority of these cytokines. This finding not only confirms the efficacy of EVs as a therapeutic agent but also highlights the enhanced potential of nanoencapsulation with alginate. Beyond preserving the bioactivity of these vesicles, nanoencapsulation offers additional advantages, including improved delivery efficiency, targeted release, and increased stability of EVs. These attributes collectively enhance the therapeutic applicability of EVs, making them a promising strategy for the treatment of inflammatory conditions. The successful application of nanoencapsulated EVs opens new horizons in both human and veterinary medicine. In human medicine, this technology could revolutionize the treatment of chronic inflammatory diseases, autoimmune disorders, and even certain types of cancer, by providing a targeted, efficient, and less invasive treatment option. The ability to modulate specific cytokines responses offers a precision medicine approach, potentially reducing the side effects associated with traditional therapies. In veterinary practice, this technology promises to enhance the treatment of inflammatory conditions in animals, including atopic dermatitis in dogs, which shares similarities with human conditions. The use of canine-derived mesenchymal stem cells for EVs production could facilitate a more species-specific therapy, potentially offering a higher efficacy and lower risk of adverse reactions. Additionally, the non-invasive nature of exosome therapy could improve animal welfare by reducing the stress and discomfort associated with conventional treatments. Overall, the advancement of nanoencapsulation technology for exosome delivery represents a significant leap forward in the development of novel therapeutic strategies. Its application across human and veterinary medicine not only broadens the scope of treatable conditions but also underscores the importance of cross-disciplinary research in advancing healthcare solutions for all species.

5 Declarations

5.1 Competing Interests

The authors declared that there is no conflict of interest regarding the publication of this manuscript.

5.2 Publisher's Note

AIJR remains neutral with regard to jurisdictional claims in published institutional affiliations.

How to Cite this Article:

Dutra *et al.*, "Exploring Extracellular Vesicles Nanocapsules in Hydrogel Delivery for Canine Atopic Dermatitis: An Anti-Inflammatory Approach", *Adv. Nan. Res.*, vol. 8, no. 1, pp. 1–17, Dec. 2024. https://doi.org/10.21467/anr.8.1.1-17

References

[1] W. Villalobos and L. Beltrán, "Importância da barreira epidérmica na dermatite atópica canina: Revisão," *Pubvet*, vol. 10, no. 7, pp. 560–567, Jul. 2016, doi: https://doi.org/10.22256/pubvet.v10n7.560-567.

[2] M. S. Kim *et al.*, "Canine amniotic membrane-derived mesenchymal stem cells ameliorate atopic dermatitis through regeneration and immunomodulation," *Veterinary Research Communications*, vol. 47, no. 4, pp. 2055–2070, Jul. 2023, doi: https://doi.org/10.1007/s11259-023-10155-5.

[3] M. M. R. E. Niza, N. Félix, C. L. Vilela, M. C. Peleteiro, and A. J. A. Ferreira, "Cutaneous and ocular adverse reactions in a dog following meloxicam administration," *Veterinary Dermatology*, vol. 18, no. 1, pp. 45–49, Feb. 2007, doi: https://doi.org/10.1111/j.1365-3164.2007.00566.x.

[4] J. P. Zanon, L. A. Gomes, G. M. M. Cury, T. D. C. Teles, and A. P. da C. V. Bicalho, "Dermatite atópica canina," *Semina: Ciências Agrárias*, vol. 29, no. 4, p. 905, Aug. 2008, doi: https://doi.org/10.5433/1679-0359.2008v29n4p905.

[5] M. S. Kim *et al.*, "Canine amniotic membrane-derived mesenchymal stem cells ameliorate atopic dermatitis through regeneration and immunomodulation," *Veterinary Research Communications*, vol. 47, no. 4, pp. 2055–2070, Jul. 2023, doi: https://doi.org/10.1007/s11259-023-10155-5.

[6] A. Sasaki *et al.*, "Canine mesenchymal stem cells from synovium have a higher chondrogenic potential than those from infrapatellar fat pad, adipose tissue, and bone marrow," *PLOS ONE*, vol. 13, no. 8, p. e0202922, Aug. 2018, doi: https://doi.org/10.1371/journal.pone.0202922.

[7] R. N. Bearden, S. S. Huggins, K. J. Cummings, R. Smith, C. A. Gregory, and W. B. Saunders, "In-vitro characterization of canine multipotent stromal cells isolated from synovium, bone marrow, and adipose tissue: a donor-matched comparative study," *Stem Cell Research & Therapy*, vol. 8, no. 1, Oct. 2017, doi: https://doi.org/10.1186/s13287-017-0639-6.

[8] H. Kalra, G. P. C. Drummen, and S. Mathivanan, "Focus on Extracellular Vesicles: Introducing the Next Small Big Thing," *International Journal of Molecular Sciences*, vol. 17, no. 2, p. 170, Feb. 2016, doi: https://doi.org/10.3390/ijms17020170.

[9] A. Akbari *et al.*, "Free and hydrogel encapsulated exosome-based therapies in regenerative medicine," *Life Sciences*, vol. 249, p. 117447, May 2020, doi: https://doi.org/10.1016/j.lfs.2020.117447.

[10] Q. Shi *et al.*, "GMSC-Derived Exosomes Combined with a Chitosan/Silk Hydrogel Sponge Accelerates Wound Healing in a Diabetic Rat Skin Defect Model," *Frontiers in Physiology*, vol. 8, Nov. 2017, doi: https://doi.org/10.3389/fphys.2017.00904.

[11] K. Zhang *et al.*, "Enhanced Therapeutic Effects of Mesenchymal Stem Cell-Derived Exosomes with an Injectable Hydrogel for Hindlimb Ischemia Treatment," vol. 10, no. 36, pp. 30081–30091, Aug. 2018, doi: https://doi.org/10.1021/acsami.8b08449.

[12] A. K. Riau, H. S. Ong, G. H. F. Yam, and J. S. Mehta, "Sustained Delivery System for Stem Cell-Derived Exosomes," *Frontiers in Pharmacology*, vol. 10, p. 1368, 2019, doi: https://doi.org/10.3389/fphar.2019.01368.

[13] F. N. Faruqu *et al.*, "Membrane Radiolabelling of Exosomes for Comparative Biodistribution Analysis in Immunocompetent and Immunodeficient Mice - A Novel and Universal Approach," *Theranostics*, vol. 9, no. 6, pp. 1666–1682, 2019, doi: https://doi.org/10.7150/thno.27891.

[14] D. Ghosh, Taposi Trishna Neog, R. Patra, K. Nath, and K. Sarkar, "Alginate Based Scaffolds in Tissue Engineering and Regenerative Medicine," pp. 389– 423, Jan. 2023, doi: https://doi.org/10.1007/978-981-19-6937-9_15.

[15] M. C. Eisenschenk, P. Hensel, M. N. Saridomichelakis, C. TamamotoMochizuki, C. M. Pucheu-Haston, and D. Santoro, "Introduction to the ICADA 2023 canine atopic dermatitis pathogenesis review articles and updated definition," *Veterinary Dermatology*, vol. 35, no. 1, pp. 3–4, Feb. 2024, doi: https://doi.org/10.1111/vde.13183.

[16] O. G. De Jong, B. W. M. Van Balkom, R. M. Schiffelers, C. V. C. Bouten, and M. C. Verhaar, "Extracellular Vesicles: Potential Roles in Regenerative Medicine," *Frontiers in Immunology*, vol. 5, Dec. 2014, doi: https://doi.org/10.3389/fimmu.2014.00608.

[17] J. J. Engel *et al.*, "Dexamethasone attenuates interferon-related cytokine hyperresponsiveness in COVID-19 patients," *Frontiers in Immunology*, vol. 14, Aug. 2023, doi: https://doi.org/10.3389/fimmu.2023.1233318.

[18] Q. Wang, B. Xu, K. Fan, J. Wu, and T. Wang, "Inflammation suppression by dexamethasone via inhibition of CD147-mediated NF-κB pathway in collagen-induced arthritis rats," *Molecular and cellular biochemistry*, vol. 473, no. 1–2, pp. 63–76, Jun. 2020, doi: https://doi.org/10.1007/s11010-02003808-5.

[19] S. N. Shirley, A. E. Watson, and N. Yusuf, "Pathogenesis of Inflammation in Skin Disease: From Molecular Mechanisms to Pathology," *International Journal of Molecular Sciences*, vol. 25, no. 18, pp. 10152–10152, Sep. 2024, doi: https://doi.org/10.3390/ijms251810152.

[20] A. Heetfeld *et al.*, "Challenging a paradigm: skin sensitivity to sodium lauryl sulfate is independent of atopic diathesis," *British Journal of Dermatology*, vol. 183, no. 1, pp. 139–145, Nov. 2019, doi: https://doi.org/10.1111/bjd.18564.

[21] J. Bestman-Smith, Jocelyne Piret, André Désormeaux, M. J. Tremblay, R. F. Omar, and M. G. Bergeron, "Sodium Lauryl Sulfate Abrogates Human Immunodeficiency Virus Infectivity by Affecting Viral Attachment," *Antimicrobial Agents and Chemotherapy*, vol. 45, no. 8, pp. 2229–2237, Aug. 2001, doi: https://doi.org/10.1128/aac.45.8.22292237.2001.

[22] M. Corazza and A. Virgili, "Allergic contact dermatitis from ophthalmic products: can pre-treatment with sodium lauryl sulfate increase patch test sensitivity?," *Contact Dermatitis*, vol. 52, no. 5, pp. 239–241, May 2005, doi: https://doi.org/10.1111/j.0105-1873.2005.00606.x.

[23] R. Kakarla, J. Hur, Y. J. Kim, J. Kim, and Y.-J. Chwae, "Apoptotic cellderived exosomes: messages from dying cells," *Experimental & Molecular Medicine*, vol. 52, no. 1, pp. 1–6, Jan. 2020, doi: https://doi.org/10.1038/s12276-019-0362-8.